

Formation of the micro-sized grains under influence of the nanosecond laser pulses

R. Miedzinski · Jean Ebothé · M. Oyama ·
I. V. Kityk

Received: 31 July 2007 / Accepted: 12 November 2007 / Published online: 22 February 2008
© Springer Science+Business Media, LLC 2008

Abstract The occurrence of a periodic photo-induced grating having about 3.2-μm period and modulation heights up to 150 nm is discovered here under the irradiation of 10-ns 1,064-nm laser pulses with Ag nano-particles deposited on ITO substrates. It is shown that the main role is played by the ITO resistance. This can be explained as the result of interaction between two coherent waves. The first wave is engendered by the fundamental laser and the second one is due to the two-photon absorption phenomenon. It is important mentioning that the observed photo-induced grating is obtained only from a treatment by single 10-ns laser pulses with an effective pump power below 0.7 GW/cm². Since the laser power densities are markedly low and the pulse durations larger than those of the femtosecond laser, the origin of this result is expected to be ascribed to the plasmon excitation leading to further thermoionization.

Introduction

It is well known that nonlinear optical effects and particularly the second-order ones can be enhanced in metallic nano-

particles [1, 2]. Actually, the second harmonic generation (SHG) at interfaces is substantially enhanced by the surface plasmon resonance (SPR) which induces at the same time a local field effect and a fluctuation in the density of oscillatory electrons at metallic interfaces. The outer interface mode resulting from both the basic and the double frequency is more sensitive to the metallic nanoparticle (NP) wall thickness. Moreover, the SPR frequency and the local field intensity can be modulated by varying the dielectric constant. As a consequence, the position and the intensity of the nonlinear optical maxima can be tuned. Accordingly, one can expect that the excitation of nano-particles in the vicinity of the SPRs can be an effective tool for a real nonlinear optical interaction between the fundamental and the second harmonic waves. For Ag nano-particles, this situation is very convenient because they have a SPR wavelength at about 520–530 nm, which corresponds to the SHG of the Nd-YAG laser. The nanoparticle size and the inter-particle distances play the main role for such kind of nonlinear optical effects [3]. It can be deduced that for an effective two-wave interaction, the resistivity of the ITO substrate and the power density at the particular point of the photo-induced Ag nano-particles have the predominant role. Due to the Gaussian-like profile of the Nd-YAG laser beam, one can expect that there exists a possibility to obtain different nonlinear interactions between the fundamental and the doubled frequency beams at the different points of the incident beam. So the expected grating should be different, which could be detected by the measurements and imaging of atomic force microscopy (AFM).

Experimental

The Ag nano-particles were prepared by a seed-mediated growth method described elsewhere [4]. The ITO film on

R. Miedzinski · I. V. Kityk (✉)
Institute of Physics, J. Dlugosz University, Al Armii Krajowej
13/15, Czestochowa, Poland
e-mail: i.kityk@ajd.czest.pl

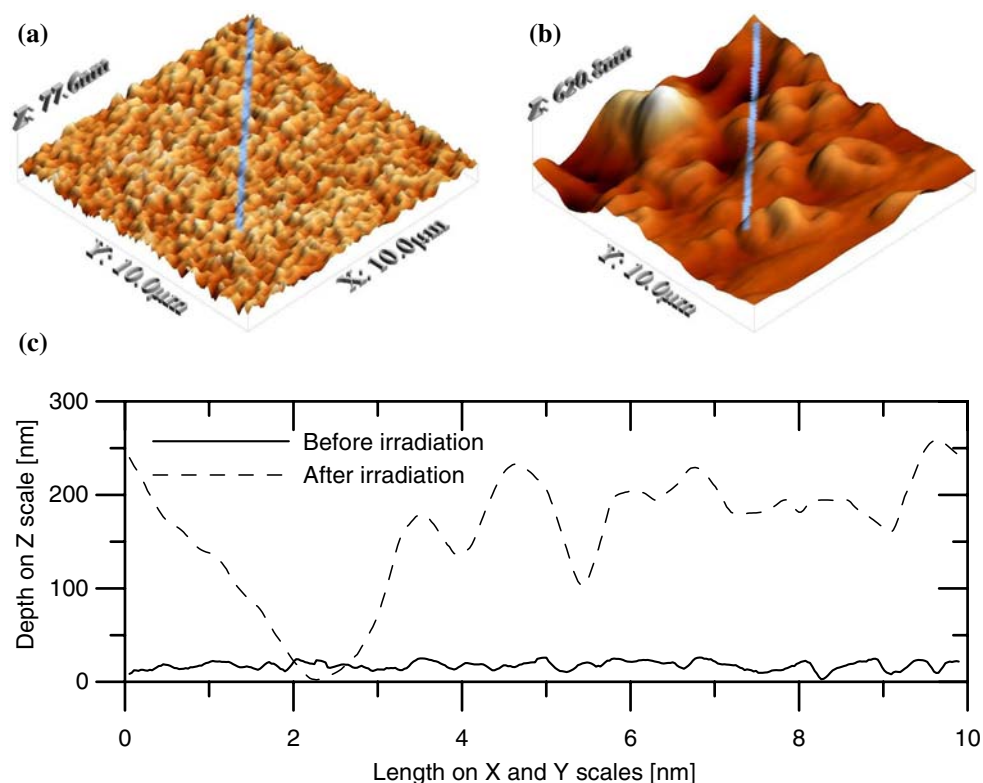
R. Miedzinski · J. Ebothé (✉)
LMEN, E. A. 3799, UFR Sciences, Université de Reims,
B. P. 138, 51685 Reims, France
e-mail: jean.ebothe@univ-reims.fr

M. Oyama
International Innovation Center, Kyoto University, Nishikyo-ku,
Kyoto 615-8520, Japan

glass substrate was ordered from Ashahi Beer Optical Ltd. Treated ITO samples were immersed in the growth seed solution and left for 24 h. This procedure leads to the formation of Ag nano-particles attached on ITO. The system is afterwards removed from the growth solution and washed several times in pure water.

In nonlinear optical measurements the samples are irradiated by 10-ns pulsed Nd:YAG laser with pulse frequency of about 10 Hz with maximal energy up to 12 mJ. By varying the spot diameter in the interval 0.2–1.00 mm, we have found that the optimal power density reaches 0.7–0.9 GW/cm². The beam presents a Gaussian profile and its polarization is changed by the Glahn polarizers. The effective irradiated sample surface has a diameter of about 0.36 mm. We used the “z-scan” technique for that. The laser beam is focused by +50-mm biconvex lens and the samples are maintained near the focal point. The absorption spectra before and after irradiation are recorded by means of the Ocean Optics HR4000 spectrometer, and they show that main changes (up to 30%) were observed at 480 nm–530 nm wavelengths, which correspond to the SPRs. The AFM imaging and measurements are obtained from a standalone SMENA NT MDT microscope used in a constant contact force mode. The images are collected in ambient atmosphere under a digitization of 512 × 512 pixels and a scanning frequency of about 1 Hz. A commercial Si₃N₄ tip of nearly 20-nm apex radius is related to a cantilever of 0.12-N m⁻¹ spring constant.

Fig. 1 Typical AFM surface topologies: (a) before irradiation; (b) after irradiation; (c) surface profiles of AgNP on ITO substrate: -solid line-before irradiation; -dashed line after irradiation



Results and discussion

The appearance of the photo-induced microscopic grains after the irradiation of the 0.5 GW/cm² laser pulses is presented in Fig. 1b as observed by AFM. The tremendous surface modification obtained can be evaluated by comparing with the image of the non-irradiated sample shown in Fig. 1a. The general sample surface profiles before and after irradiation as depicted in Fig. 1c clearly reveal the real change induced by that treatment. The quantitative parameters of the film topography summarized in Table 1 confirm the importance of the change observed. This effect was firstly observed with the nanosecond laser pulses and could be used for the following photo-induced treatment of the Ag nano-particles. It is well known that the irradiation of the composites containing Ag nano-particles by femtosecond laser pulses occurs with a light peak intensity up to 0.2 TW/cm² at 400 nm. We have investigated the role of the substrate resistivity, the type of metallic nano-particles and the laser wavelengths on the photo-induced operation and examined the change of the sample's morphology by AFM imaging.

From Fig. 2, one can see that after illumination by a single pulse of the AgNPs grown on ITO of about 50-Ω/sheet resistivity, there occurs a substantial widening of the surface morphology whatever be the size of sample-analysed surface. This modification results from a superposition of the local laser heating and the large amount of free carriers

Table 1 Topology characteristics of the photo-induced grating obtained by AFM testing of different beam-induced places of the materials as related to Fig. 1c

Calculated magnitude	Before irradiation (nm)	After irradiation (nm)
RMS roughness	5.64	56.01
Average height	29.36	173.4
Maximum height	77.59	306.9

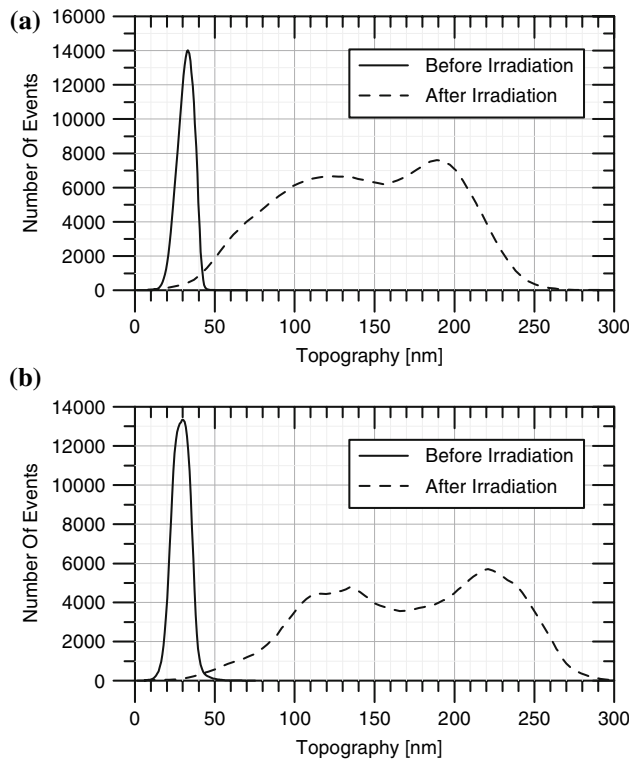


Fig. 2 The height distribution on the irradiated and non-irradiated AgNP on ITO substrate: (a) topography taken at $(25 \times 25 \mu\text{m})$ length scale; (b) topography taken at $(10 \times 10 \mu\text{m})$ length scale

induced by the laser. Depending on the substrate surface resistivity, different regimes of the photo-induced carrier kinetics are involved. The higher resistivity restrains the disappearance of the photo-induced charges and favours their trapping on the different interface local states. At the same time, irradiation by the 1,064-nm light permits the formation of two waves: the first one being the fundamental and the second one of doubled frequency—at 532 nm. These two waves interfere, engendering several modifications of the surface relief. As a consequence, when equilibrium between the photo-induced carriers and their scattering by the lattice sub-systems is optimal, one can achieve the regime of interference between the fundamental and the doubled frequency beams. The main role here is played by the occurred plasmon resonance waves having wavelengths

of about 520 nm. This wavelength is located near the one of the SHG. This is the reason why the periodic morphology shown in Fig. 3 is observed only for the fundamental 1,064-nm wavelength and why it is absent during the excitation by the 532 nm itself. In the last case there exists only one wave because the second one is effectively absorbed by the material.

Another interesting fact is presented in Fig. 4. It is clearly seen that depending on the beam profile and AFM scanning at the different points of the sample one can measure the heights and periodicity of the photo-induced grating (see Table 2). This fact is a consequence of different interactions between the fundamental laser beam and the doubled frequency resonances effectively interacting with the fundamental wavelengths.

All the optical transitions from the ground state to the excited states as well as the transitions from the excited states are due to the interactions with the lattice or disordered matrix vibrations. However, in the strength field external light, mechanical, magnetic or internal different impurities with large radius such as voids begin to play another particular role of higher electron-phonon interactions which presents the extension of the Hook rule. Why this term should play a special role? Because it possesses the symmetry described by the third rank polar tensor, the same by which are described the effects such as piezoelectricity, SHG and electro-optics ones. Moreover, in materials without any inversion centres these terms are of particular importance, because they may become an efficient tool for the formation of the non-centro-symmetry in a medium randomly oriented at initial stage. The use of external electrical fields with a defined polarization allows to form a stimulated local non-centro-symmetry. Its values should be proportional to the third space derivatives of the potential following the extension of the Hook rule. So, to have the possibility of observing the effects described by the third-rank polar tensors like piezoelectricity, linear electro-optics or SHG, it is necessary to have a sufficiently large strength of the external field and a considerable third rank derivatives of the electrostatic field potential. Therefore, an appropriate choice of the covalence degree can lead to the existence of the optical SHG. Another important factor is the energy of the photo-stimulated phonons, particularly their matching with the phase conditions. Because the energy of the phonons in the disordered materials forms almost the continuous spectrum, one can expect to find at least one frequency to satisfy the phase matching with the phonon participation. In that case, both the electron charge density asymmetry and the resonance frequency electron-phonon conditions would play a substantial role. These effects are originated from the transitions between pure electronic and electron-vibration states due to the anharmonic electron-phonon interactions [5, 6]. One of main

Fig. 3 AFM-3D visualization of irradiated and non-irradiated ITO:Ag surfaces: **(a)** the morphology before illumination; **(b)** after illumination by the 1,064-nm Nd-YAG laser pulses; **(c)** and **(d)** correspond to the same as **(a)** and **(b)** with higher space resolution

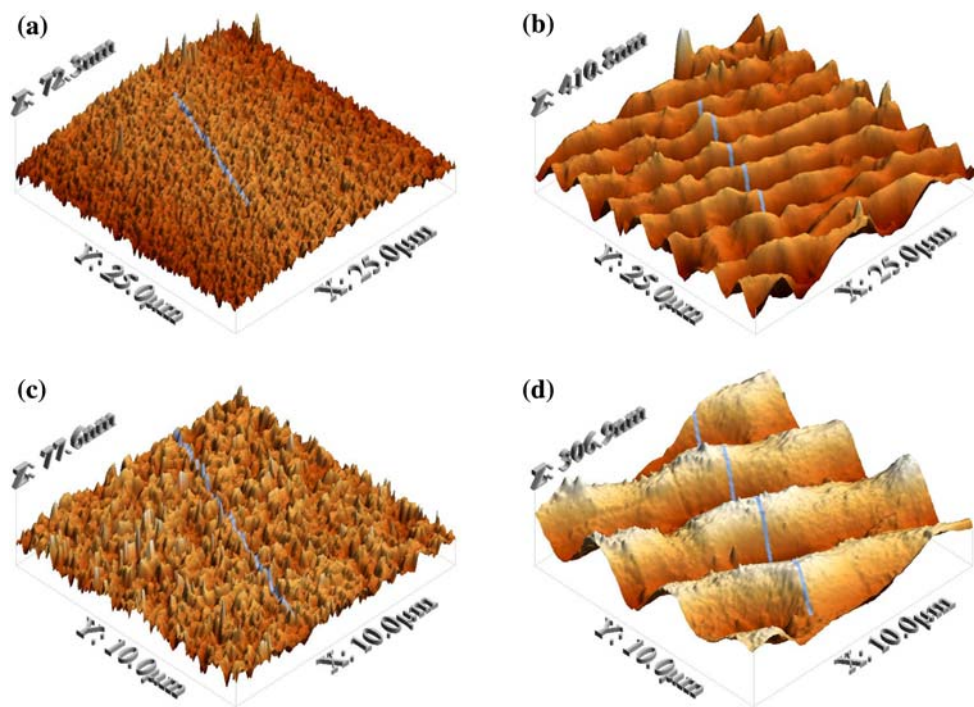
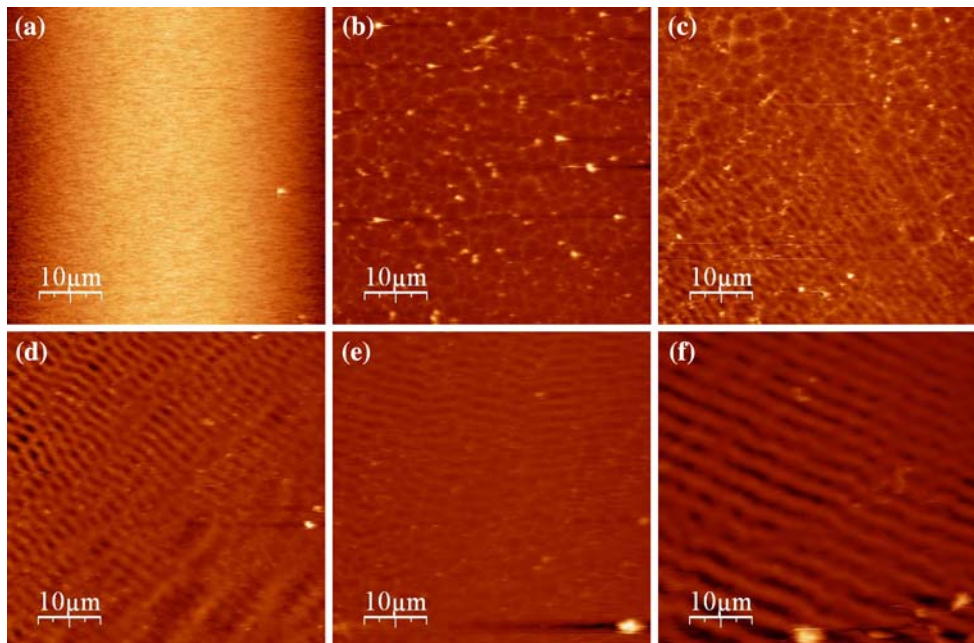


Fig. 4 Pictures **(a)**: Display of the non-irradiated surface of AgNP on ITO substrate; **(b)** at point 0.2 mm from the beam spot borders; **(c)** at point 0.4 mm from the beam spot borders; **(d)** at point 0.7 mm from the beam spot borders; **(e)** at point 0.95 mm from the beam spot borders; **(f)** at point 1.1 mm from the beam spot borders



requirements of the ITO substrate is that the regime of the photo-induction should be chosen to be below the melting point. At the same time, it should form a lot of photo-induced metastable crystallite states with the non-centro-symmetry. This may be achieved only by the excitation of the phonon modes described by the third-rank polar tensors linked to the second-order optical susceptibilities. So, one can say about some specific photo or short time thermo-phase transitions. It is well known that all the phase

transitions with temperature are described within a model of the condensation of the soft phonon modes or, simply but one of the condensations of the anharmonic phonon modes in the metastable polaron potential is responsible for the acentricity of the medium.

Semi-conducting materials including ITO possess several structural instability phases at many temperatures (pressures) which on the language of the microscopic description present an enhanced number of anharmonic

Table 2 Topology characteristics of the photo-induced grating obtained by AFM testing of different beam-induced places of the materials as related to Fig. 4

Sample labelization	RMS roughness (nm)	Average height (nm)
(a)	10.04	30.43
(b)	15.65	63.39
(c)	10.13	47.66
(d)	15.13	82.55
(e)	18.63	128.79
(f)	63.42	201.27

phonon modes. From a mathematical point of view, anharmonic phonon modes occur due to the extension of the Hook rule under the influence of external vector potential, and the phenomenological approach is described by the third-rank polar tensors. From the viewpoint of solid state theory, they should be considered in the optical spectra as the broadening and shift of the spectral lines, the different kinds of Jahn-Teller effects, the spin-oriented alloys or the quasi-liquid phase. Experimentally they are always determined in the Debye-Waller factor of the X-ray spectra. The effects like electro-optics or piezo-optics usually exist within the framework of the anharmonic phonon oscillators.

Following the results presented above, one can conclude that these modes are crucial in the investigation of materials possessing the inversion symmetry and when we have a breaking of the non-Centro symmetry. This conception begins to be very productive, even for the chiro-optical phenomena, surfaces, etc. However, for the non-centro-symmetrical media these interactions may affect the intermolecular charge transfer and the occupation of the electron-phonon states (polaron ones) [7, 8]. A large amount of such phonons particularly exist near the so-called van Hove singularities, near the Fermi energy levels. Many critical phenomena like superconductivity are considered within this conception. Moreover, one can expect that the bounded polaron states from the processes of the free carrier that are excited by light and the formation of charged defect states play a substantial role in the effects.

A typical role in such a phenomena may also be played by the nano-confined states possessing a large amount of nano-quantized states in the forbidden gap regions.

Now a lot of experiments confirmed the existence of the giant photo-thermal irreversible effects in glasses, polymers, etc. Moreover, the changes of Raman modes and sometimes even the ones of FTIR spectra concur with the observed hypothesis. Of course, within the phenomenological approach one can introduce effective polarizabilities without distinction in the role of electron and phonon sub-systems and considering the material

like a homogenous phase. In that case, in many processes such as kinetics or temperature dependences, structural instabilities remain unclear. In general, these processes are considered within the differential first-order equations of thermo-diffusion and thermo-conductive transport within the intra-molecular electron charge transfer, charging of the vacancies' defects and carrier transport. In most cases, this is enough to explain this dependence. However, this approach is not compatible with the solid-state approach, where the material search begins from the search of the relatively unstable phase by DSC and other methods.

The results obtained here may be explained as a consequence of interaction between two coherent waves. The first one-fundamental originated from the fundamental laser and the second one due to the two-photon absorption. It should be pointed out that the observed photo-induced grating is obtained only for the treatment by single 10-ns laser pulses with an effective pump power below 0.7 GW/cm^2 . It is necessary to add that better grating effect was achieved for s-laser polarization. Changes of the frequency repetition do not influence the observed effect.

Our recent experiments have shown that during the illumination by both single as well as bicolour treatment, the grating occurs with the structure but disappears after the switching off the external optical fields. The thermal effects, which in the microscopic-level language play a substantial role, should be evidenced in both cases only by their relaxation and particularly in the treatment by the IR light. One can say that the decaying processes of the anharmonic phonons could lead to formed grating. This work along with the time-resolved temperature measurements may assist to clarify the origin of the effect. They are described by the Hamiltonian operator linked to electronic, vibration, electron-vibration subsystems, and the corresponding states are the eigen-energies of the total Hamiltonian. Despite the effects of the SHG, several contributions here give the hyper-Raman and multi-phonon states, which participate in the effects. One of the possible methods to look at these effects consists in the delaying of the optically induced signal with respect to the probing beams. However, getting it in the pure form remains a technical challenge since we always have the contribution of both the electronic and the phonon sub-systems.

The observed effect was maximal for the surface resistivity $50\text{-}\Omega/\text{sheet}$ and was substantially lower for the resistivity equal to about $4\text{-}\Omega/\text{sheet}$. This may be explained by the substantial role of the photo-induced free carriers of the plasmon origin which are gating by the substrates. Additional experiments are planned to clarify the role of the carriers.

The absence of effect for the 530-nm illuminated wavelength may indicate the main role of interaction

between the input fundamental wavelength and its second harmonics. The second harmonic wavelength for the 530 nm hits the absorption spectral range, and this may confirm the fact that the coherent bicolour interference plays the main role in the observed phenomenon. This is particularly different from the two-beam grating observed in Ref. [9], where the grating mechanism is based on the holographic interactions of the two coherent beams. One has here less dependence on the beam polarization and the incident angle of the irradiating beams for the single-beam treatment.

Conclusion

We have established that during illumination of the silver nano-particles by the single pulses of the 10 ns Nd-YAG and laser pulses at wavelength 1,064 nm there is a marked morphological change of the material surface. The occurrence of periodic photo-induced grating of about 3,200-nm period and modulation heights up to 150 nm is revealed with Ag nano-particles deposited on ITO substrates under the irradiation of the 1,064-nm laser pulses. It is shown that the main role is played by the resistance of the ITO substrate. This may be explained as a consequence of interaction of two coherent waves. The first one-fundamental originated from the fundamental laser and the

second one due to the two-photon absorption phenomenon. It clearly appears here that the observed photo-induced grating is obtained only by the treatment with single 10-ns laser pulses of effective pump power below 0.7 GW/cm². The main mechanism responsible for such periodic relief is a superposition of the fundamental wavelength at 1,064 nm and its doubled frequency signal. Additional important factor is determined by the electro-lattice sub-system operating by transport transfer.

References

1. Karpov SV, Gerasimov VS, Isaev IL, Podavalova OP, Slabko VV (2007) *Colloid J* 69:159
2. Zhu X (2007) *Nanotechnology* 18:225702
3. Lecler S, Haacke S, Lecong N, Cregut O, Rehspringer JL, Hirlimann C (2007) *Opt Express* 15:4935
4. Kityk IV, Umar A, Oyama M (2005) *Physica E: Low-dimen Syst Nanostruct* 27:420
5. Kityk IV, Golis E, Filipecki J, Wasylak J, Zacharko VM (1995) *J Mater Sci Lett* 14:1292
6. Kityk IV, Makowska-Janusik M, Gondek E, Krzeminska L, Danel A, Plucinski KJ, Benet S, Sahraoui B (2004) *J Phys: Cond Mat* 16:231
7. Malynych S, Chumanov G (2003) *J Amer Chem Soc* 125:2896
8. Evanoff DD Jr, Chumanov G (2005) *Chem Phys Chem* 6:1221
9. Syvenkyy Yu, Kotlyarchuk B, Savchuk V, Zaginey A, Dabos-Seignon S, Derkowska B, Lychak O, Sahraoui B (2007) *Opt Mater* 30:380